Atmospheric Pollution Research 14 (2023) 101835

Contents lists available at ScienceDirect

Atmospheric Pollution Research

journal homepage: www.elsevier.com/locate/apr

Comprehensive characterization of wintertime submicron aerosol in a Nordic town influenced by residential wood combustion, traffic and industrial sources

Luis M.F. Barreira [a,*], Teemu Lepistö [b], Laura Salo [b], Aku Helin [a], Minna Aurela [a], Sanna Saarikoski [a], Niina Kuittinen [b], Topi Rönkkö [b], Hilkka Timonen [a]

[a] Atmospheric Composition Research, Finnish Meteorological Institute, 00101, Helsinki, Finland
[b] Aerosol Physics Laboratory, Physics Unit, Faculty of Engineering and Natural Sciences, Tampere University, 33014, Tampere, Finland

ARTICLE INFO

Keywords:
Wintertime air quality
Northern latitude
Chemical composition
Lung deposited surface area
Sources contribution

ABSTRACT

Anthropogenic particulate matter with sizes smaller than 1 μm (PM_1) is a concerning air pollutant that can affect human health. In this study, we present PM_1 measurements performed in a small town in northern Finland that is exposed to contrasting sources (residential wood burning, traffic, industrial activities). The study was conducted in winter 2021, with a mobile laboratory equipped with sophisticated on-line aerosol instrumentation. The results showed a significant increase in particulate mass and number concentrations from biomass burning in residential areas and town centre due to the high share of residences using biomass burning. Organics and equivalent black carbon (eBC) clearly dominated the PM_1 composition during the highest pollution levels, followed by inorganics (sulfate, nitrate and ammonium). PAHs and a few elements (e.g. K, Cl, Zn) were as well higher during evening. A source apportionment confirmed the association between high PM_1 values and biomass burning, even though the traffic contribution was also important. PM_1 measurements at an industrial area showed an increase in sulfate, organics, eBC, and a few elements (e.g. Cl, Na, Fe), and characteristic size distributions. Simultaneous measurements of lung deposited surface area (LDSA) of particles showed the source-specificity of biomass burning, traffic and industrial emissions on LSDA size distributions. Overall, the results enlighten the impact of relevant pollution sources on Nordic towns air quality during the coldest months and show the importance to also consider the chemical composition, particle numbers, and LDSA in future air quality metrics.

1. Introduction

Air quality is one of the most critical problems facing humanity. The rapid economical and industrial developments over the past century have caused an increase in the production of pollutants and their emissions into the atmosphere, with a consequent decrease in air quality (e.g. Chan and Yao, 2008). Poor air quality is responsible for a significant share of annual morbidity and mortality around the world due to several respiratory, cardiovascular, immune, and nervous system diseases (e.g. Brauer et al., 2021; Varghese et al., 2022). In 2019, air pollution accounted for an estimated 6.7 million deaths that is about 12% of all deaths registered in the same year (Brauer et al., 2021). Currently, almost the entire world's population (99%) lives in places where air quality levels exceed WHO recommendation limits for particulate matter (WHO, 2022).

The air quality is greatly impacted by the chemical and physical properties of atmospheric particulate matter (PM), even though technological developments and legislation have been implemented in the past decades to reduce PM emissions. These chemical and physical properties are highly variable over time due to changes e.g. in source intensity, atmospheric conditions, and regional characteristics such as geographic location (e.g. Barreira et al., 2021). PM is composed of a complex mixture of chemical constituents, such as organic species, inorganic salts, black carbon (BC), metals, and other constituents, which are originated from many different biogenic and anthropogenic sources (Chen et al., 2022; e.g. Pan et al., 2022). From organic constituents,

Peer review under responsibility of Turkish National Committee for Air Pollution Research and Control.
* Corresponding author.
E-mail address: luis.barreira@fmi.fi (L.M.F. Barreira).

https://doi.org/10.1016/j.apr.2023.101835
Received 22 May 2023; Received in revised form 3 July 2023; Accepted 3 July 2023
Available online 6 July 2023

polycyclic aromatic compounds (PAHs) and a group of compounds commonly called by BTEX (benzene, toluene, ethylbenzene and xylenes) are of particular concern to human health, being among the priority pollutants list in European Union and US Environmental Protection Agency (EPA) due to their carcinogenic and mutagenic properties. Typically, benzo(a)pyrene is chosen as a tracer for PAH compounds, but fragments of PAH compounds measured by mass spectrometer instruments have been as well used as a proxy for these polyaromatic compounds (Lee et al., 2023; e.g. Ye et al., 2017). BC emissions can also have a negative impact on health and environment, even though they are currently underregulated (e.g. Tiwari et al., 2021). In addition, particulate metals are of concern since some of these elements can have several toxicological effects even at trace concentrations (e.g. Wani et al., 2015).

Furthermore, aerosol particle size distribution is important in terms of air quality. Most urban air particles are ultrafine (≤100 nm), which have been linked with deteriorating effects on human health such as changes in inflammatory and cardiovascular conditions (Hakkarainen et al., 2022; e.g. Ohlwein et al., 2019). The lung deposited surface area (LDSA) is a metric that estimates the surface area concentration of particles that deposit in the alveolar region of the human respiratory tract. Even though this metric does not provide toxicological information of measured particles, it is considered relevant to predict the negative health effects of aerosol particles since an association between LDSA and health issues has been previously reported (e.g. Aguilera et al., 2016; Patel et al., 2018). Once particles deposit in the alveolar region, they can both cause local pulmonary effects and enter the blood stream, potentially affecting the function of several vital organs e.g., the human brain (Heusinkveld et al., 2016). Therefore, ultrafine particles can contribute notably to LDSA despite contributing poorly to PM mass compared to bigger particles. In fact, in a recent study, the percentage of particle mass that deposits in lungs was higher in Helsinki than in the capital region of Delhi due to the smaller median particle size (Salo et al., 2021). The monitoring of ultrafine particles with particle number (PN) concentration has been recently introduced in the WHO air quality guidelines as a good practice statement (WHO, 2021).

In this study, the chemical and physical properties of PM_1 in ambient air were investigated during winter in a small town (Raahe) located in northern Finland and exposed to contrasting local aerosol pollution sources (e.g. biomass burning, traffic, industry). A mobile laboratory containing a variety of sophisticated instruments was used to carry out measurements at different locations and during different times of the day to study the time-dependent contribution of pollution sources to PM_1 properties. The study allowed to understand how the separate pollution sources influence differently the PM_1 chemical composition, size distributions, and LDSA concentration.

2. Experimental section

2.1. Measurement sites

Comprehensive online PM_1 measurements were performed in Raahe (64°41′N 24°29′E, 8 a.s.l.), northern Finland, from 25th of January to February 4, 2021. Raahe is a small town with about 25 000 inhabitants. The town has several PM_1 emission sources, including detached-housing residential areas; a relatively large industrial area located in the southwest (approx. 4 km away of the town centre); a highway (E8); and one of the busiest ports by cargo tonnage in Finland. The measurements were carried out in the town centre, residential areas, the industrial area and on the highway with a mobile laboratory (see e.g. Lepistö et al., 2022; Rönkkö et al., 2017) to evaluate the contribution from the separate sources to PM_1 properties (chemical composition, particle size distributions, and LDSA).

The residential areas included Lapaluoto (Res I), Varvi (Res II), and Velkaperä (Res III) (Fig. S1), which are all detached-housing areas. Res III (Velkaperä) uses both district heating and biomass burning for residential heating, while Res I and Res II (Varvi and Lapaluoto) rely predominantly on biomass burning. The centre of the town contains apartment buildings and communal services in addition to detached-housing residences using both district heating and biomass burning. The traffic-environment measurements were performed at the E8 highway. In addition, measurements were conducted in the industrial area. Furthermore, background aerosol concentration and properties were measured in Siniluoto (approx. 2 km south from the industrial areas and 6 km from the town centre). However, the background site was occasionally exposed to PM emissions from the previously mentioned areas due to regional transport.

The differences between areas were studied by driving three measurement routes. Route A included the residential areas and the town centre whereas route B included the highway and the background measurement site (Fig. S2). The industrial area route consisted of driving near different zones inside the industrial area (e.g. coal fields, harbor, furnace, smelter). Route A had a duration of approximately 20–25 min from the start to the end point and allowed to compare residential areas and town centre. Route B also lasted 20–25 min while the driving at the industrial area took 1–2 h. The measurement periods at studied locations during the campaign are shown in Fig. S3. These chosen routes and duration periods allowed to obtain a reasonable characterization of particulate matter at each location.

2.2. Instrumentation

2.2.1. Soot particle aerosol mass spectrometer (SP-AMS)

The chemical composition of PM_1 was measured by a soot particle aerosol mass spectrometer (SP-AMS; Aerodyne Research Inc, Billerica, US; Onasch et al. (2012)), which allows the on-line and fast measurement of several non-refractory (e.g. organics, nitrate (NO_3), ammonium (NH_4) and sulfate (SO_4)) and refractory (e.g. rBC and metals) PM constituents.

In this study, the SP-AMS was operated with a 15 s time-resolution in a mass spectra mode to obtain the nitrate-equivalent concentration of measured constituents (Canagaratna et al., 2007; Jimenez et al., 2003), except at the background station and on the 28th of January at the industrial area where the time resolution was 60 s. The size-range of particles detectable by the SP-AMS is approximately from 50 nm to 1 μm. The effective nitrate response factor (RF_{NO3}) and relative ionization efficiency of sulfate (RIE_{SO4}) were determined by performing an instrumental calibration to convert analyte signals into nitrate equivalent mass concentrations using dried and size-selected (300 nm of mobility diameter) ammonium nitrate and ammonium sulfate particles.

2.2.2. Aethalometer

The measurement of equivalent BC (eBC) was performed by a dual-spot aethalometer (AE33, Magee Scientific; Drinovec et al. (2015)). The AE33 allows for real-time measurement of particulate light absorption at seven different wavelengths (370–950 nm), and it compensates for filter loading artifacts and tape advancement errors when measuring eBC concentrations at 880 nm (Drinovec et al., 2015). The instrument sampling flow rate was 5 L min^{-1} and the inlet cut-off size was 1 μm (sharp cut cyclone, BGI model SCC1.197). A time resolution of 1 s was employed. A M8060 filter tape (Magee Scientific), containing tetrafluoroethylene (TFE)-coated glass fiber filters, was used.

To estimate the contribution from wood burning and fossil fuel to eBC, the source apportionment method referred as the aethalometer model was employed (Sandradewi et al., 2008). Briefly, the light absorption coefficients measured at 470 nm and 950 nm wavelengths are used to estimate the contribution of BC from biomass burning (BC_{WB}) and fossil fuel (BC_{FF}). The absorption Ångström exponent used for fossil fuel (α_{FF}) was 0.9, while the corresponding exponent for wood burning (α_{WB}) was 1.68. These values have been recommended in another study (Zotter et al., 2017).

2.2.3. Electrical low-pressure impactor

An Electrical Low-Pressure Impactor (ELPI+, Dekati Oyj, Keskinen et al. (1992), Järvinen et al. (2014)) was used for real-time particle size distribution measurements. In the ELPI+, the sampled particles are charged in a unipolar diffusion charger and classified in a cascade impactor according to their aerodynamic diameter. The impactor has 14 stages that are connected to electrometers for the measurement of electrical current as a function of particle size. The electrical current data is subsequently converted to particle number concentration. The ELPI + enables both the measurement of particle number size distributions and the determination of LDSA size distributions in the size range of 6 nm–10 μm (aerodynamic diameter) (Lepistö et al., 2020). The time resolution of ELPI + size distribution measurements was 1 s.

2.3. Data handling

The SP-AMS data was analysed with a ToF-AMS high resolution (HR) Analysis software (SQRL 1.65C and PIKA 1.25C), running in IGOR PRO 7 (Wavemetrics Inc., USA). A chemical time-dependent collection efficiency was calculated according to Middlebrook et al. (2012) to correct for losses of particles due to e.g. aerodynamic lens, widening particle beam and bouncing off the vaporizer before flash vaporization. As an exception from Middlebrook et al. (2012), a collection efficiency of 0.45 was used when ammonium concentration was below the detection limit. The limit of detection (LOD) for ammonium was determined by adding a HEPA filter to the sampling line, averaging the measured mass concentrations of ammonium using a collection efficiency of 0.5, and multiplying the resulting standard deviation by three. The obtained LOD value for ammonium was 0.03 μg m^{-3}. The LOD for organics, nitrate, and sulfate were also determined as for ammonium, and the obtained values were 0.4, 0.36, and 0.10 μg m^{-3}, respectively.

The sources of organic aerosol (OA) were investigated by Positive Matrix Factorization (PMF) analysis, using a CU AMS PMF Execute Calcs Tool v3.00 A (Ulbrich et al., 2009; Zhang et al., 2005), running in IGOR Pro 7. The number of factors studied varied between 1 and 10. Based on the evaluation of $Q/Q_{expected}$ and residuals, a 4-factors solution was selected. A validation test was also performed for the 4-factor solution by varying fpeak (delta fpeak of 0.5), and the results obtained with the different fpeak values were stable.

The concentrations of a few PAH species were estimated by selecting PAH-related ion fragments ($C_{10}H_8^+$, $C_{12}H_8^+$, $C_{12}H_{10}^+$, $C_{13}H_{10}^+$, $C_{14}H_{10}^+$, and $C_{18}H_{12}^+$) from high resolution mass spectra analysis similarly as in Herring et al. (2015). An RIE of 1.35 was employed as in Slowik et al. (2004). The individual species were then evaluated to study the source-dependency of composition and concentration of PAH species in PM_1. However, even though high-resolution data was used, other non-PAH constituents with the same molecular formula may have still contributed to the measured PAH concentrations. Therefore, the total concentration of PAHs was also determined as in Dzepina et al. (2007) from the unit mass resolution data and used for the comparison with the total concentration of the referred fragments. As for HR data, an RIE of 1.35 was employed for UMR PAH concentration. Note also that $C_{18}H_{12}^+$ has a slightly higher mass-to-charge (m/z) than the mass range of the calibration curve employed in the SP-AMS analysis (17.0027 (O^+) to 183.9509 ($^{184}W^+$)), which may impact slightly its determination.

Six elements (K, Cl, Cr, Cu, Fe, Na, V, and Zn) were detected by the SP-AMS. Some of these elements are ionized by both the laser and at the surface of the Tungsten ionizer. This makes quantitation challenging since e.g. their relative ionization efficiencies are difficult to obtain and there is a potential prolonged instrumental response that results from measurement signals during beam closed operation (Carbone et al., 2015; Salcedo et al., 2012). Therefore, the results from elements measured in this study may be interpreted as semi-quantitative. Note also that the amounts of zinc were obtained from the isotope at m/z 68 due to an overlay of its main isotope with SO_4 at m/z 64.

For most of the figures of this study, the data points were averaged over all measurement periods at studied sites (Res I-III, town centre, highway, background, and industrial area). However, AE33 and ELPI + data were pre-averaged to 15 s resolution for residential areas, town centre, highway, and industrial area, and 60 s for the background site, to match the time resolution of the SP-AMS and reduce uncertainties (except on the 28th of January at the industrial area where a time resolution of 60 s was used for SP-AMS, which was considered when pre-averaging the AE33 data since concentrations were directly compared between both instruments in the manuscript). For the source apportionment of BC (to obtain BC_{FF} and BC_{WB}; see Sect. 2.2.2), the data points were pre-averaged over the measurement period (day or evening) at the referred sites as the biomass burning percentage (BB %) used to calculate BC_{FF} and BC_{WB} is not reliable when using 15 s data.

For the determination of LDSA from ELPI + measurements, a model for particle deposition in the human respiratory tract presented in a report by International Commission on Radiological Protection (ICRP, 1994) was used as in Lepistö et al. (2020). Briefly, this model determines semi-empirically the particle deposition in respiratory tract regions. The simplified equations employed in the model can be found e.g. in Hinds and Zhu (1999) and take into consideration different parametrical values, such as gender, age, and breathing rate.

Weather data (temperature, wind speed, and wind direction) was measured at an FMI weather station located in Lapaluoto. The data is freely available for download at FMI's website.

Since the PM sources at the studied location were assumed to have distinct diurnal cycles, we divided the measured periods into day (8:00 h to 17:00 h) and evening (17:00 h to 24:00 h) times for evaluating the changes in chemical composition, source contributions, and particle number and LDSA size distributions. All data is displayed in local time (UTC+2).

3. Results and discussion

3.1. Chemical characterization of atmospheric PM_1

3.1.1. Concentration and relative contribution of major PM_1 constituents

The mean, median, and 25th and 75th percentiles of major PM_1 constituents (organics, NO_3, NH_4, SO_4, and eBC) measured during day (8:00 h to 17:00 h) and evening (17:00 h to 24:00 h) at each of the measurement locations by the SP-AMS and AE33 are represented in Table S1. The overall PM_1 composition, concentration, and corresponding atmospheric conditions (temperature, wind speed, and wind direction) over the measurement days are shown in Fig. S4. As observed in Fig. 1, the average concentration of PM_1 was about 3 times higher during evening than during daytime at the residential areas (Res I—Res III). Organics contributed the most to the high evening PM_1 concentrations, followed by eBC (Table S1). The evening-time increase in PM_1 has been previously observed at residential sites in northern Europe during the coldest months of the year, and is mostly caused by both increased biomass burning and stagnant atmospheric conditions (Glasius et al., 2018; e.g. Saarikoski et al., 2021).

Surprisingly, the evening PM_1 concentration was the highest at the town centre, with an average of 17.07 μg m^{-3} (Table S1). As for residential areas, organics and eBC clearly dominated the evening PM_1 composition at this location (Fig. 1 and Table S1). The high PM_1 during evening time at Raahe's town centre contrasts with what has been previously observed in downtown locations of capital areas where the concentrations are frequently higher during morning rush hours (Aurela et al., 2015; e.g. Barreira et al., 2021). The PM_1 levels were also higher than in the studies performed at residential areas in Helsinki during winter (Aurela et al., 2015; e.g. Teinilä et al., 2022). The most plausible explanation for the high evening PM_1 in our study is the fact that Raahe has a significant share of residences using biomass burning in the centre of the town, causing an increase in wood burning emissions, which is not seen in the downtown of the biggest northern European cities. Furthermore, the temperature at northern latitudes is on average lower,

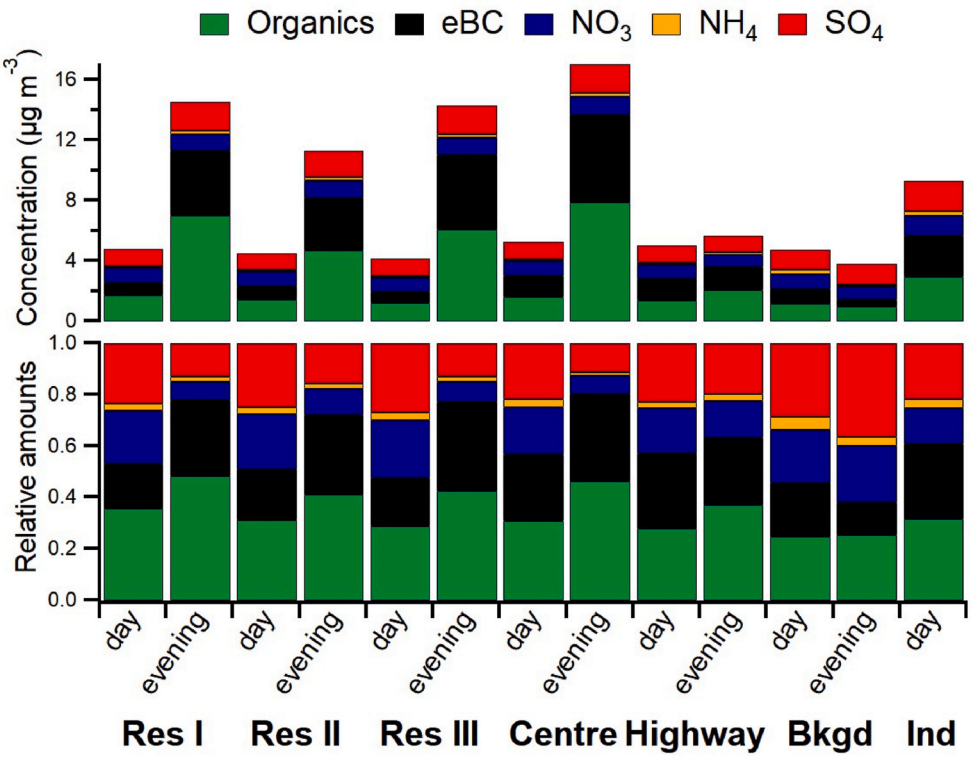

Fig. 1. Mean concentrations and relative amounts of PM_1 species (organics, NO_3, NH_4, and SO_4), measured by the SP-AMS, and of eBC measured by the Aethalometer at residential areas (Res I-III), town centre, highway, background site (Bkgd), and industrial area (Ind) during day and evening.

which promotes the intensification of biomass burning for heating purposes.

The average concentration of non-refractory inorganics (i.e. the sum of sulfate, nitrate and ammonium concentrations) was also more elevated (approx. 1.5 times) during evening at residential areas and town centre (Fig. 1 and Table S1). This result strongly suggests the existence of a local source of inorganics, especially since the increase was not observed at the background and highway sites excluding a dominant meteorological effect. Since the primary emission of inorganic aerosol from biomass burning is rather negligible, it is likely that these compounds were formed chemically from their atmospheric precursors (e.g. SO_2, NH_3, NO_x) (Souri et al., 2017).

The average evening PM_1 mass concentration at the highway was only 1.1 times higher than the concentration during daytime, likely reflecting a small effect from boundary layer height decrease in the evenings and/or a slight increase in traffic, while the average concentration at the background site was 1.2 times higher during daytime than during evening (Table S1). The daytime concentration of PM_1 at these sites was generally similar to the ones at the residential areas and town centre (Fig. 1). This result seems to indicate that local sources had a higher influence on PM_1 mass concentration during evenings than during mornings, and that the highway was a minor source of atmospheric pollutants to the inhabited areas of the town.

The PM_1 concentration inside the industrial area was the highest one from all measured sites during daytime but smaller than the evening concentrations at the residential areas and town centre (Fig. 1). Organics and eBC were the dominant PM_1 constituents inside the industrial area (Fig. 1). These constituents also had high standard deviations (Table S1), which reveals the occurrence of concentration spikes. These spikes were not observed at the other studied locations. On the other hand, the average concentration of nitrate and ammonium were relatively low. Generally, the chemical composition of PM_1 at the industrial area was similar to the one at the other sites, but the concentration of sulfate, eBC, and organics was significantly larger during daytime when industrial measurements were performed (Fig. 1 and Table S1). Note as well the high standard deviations for sulfate (Table S1), which were also not observed at other studied locations.

Large eBC or EC and organics concentrations have been previously observed in studies performed inside industrial sites, such as steel mills, even though their absolute and relative concentrations have varied significantly according to the site/activity (Dall'Osto et al., 2012; e.g. Sylvestre et al., 2017; Tsai et al., 2007). However, the concentrations of organics and eBC can have a strong contribution from vehicles circulating inside the industrial areas, especially from heavy-duty/street-maintenance vehicles (e.g. Karjalainen et al., 2019), and therefore it is not possible to determine the fraction of these compounds that is directly associated with the industrial emissions. High sulfate emissions from industrial production have also been previously reported, being inclusively the dominant particulate component e.g. in steel factories. On the other hand, the concentrations of ammonium and nitrate concentrations have been low in the mentioned studies, even though their absolute concentrations were as well highly dependent on the industrial processes.

In order to investigate the impact of industrial emissions in more detail, PM_1 concentrations at the residential area, town centre, highway and background were separated according to the northern and southern winds. The concentration of PM_1 increased at all studied sites during southern winds, especially when wind speed was moderate (Figs. S4 and S5). This result suggests that industrial emissions may have had an impact on the PM_1 chemical composition at nearby populated areas. However, southern winds only occurred during two campaign days (28th of January and 2nd of February) and for a few hours, which limited the evaluation of the influence of industrial emissions on PM_1 composition at the studied populated areas.

3.1.2. *The contribution of measured constituents to PM_1 pollution level*

The concentration and relative contribution of major PM_1 species (organics, eBC, NO_3, NH_4, and SO_4) during day and evening categorized

to different PM_1 levels are shown in Fig. 2. The concentration and relative contribution of organics and eBC clearly increased with PM_1 levels, showing a total contribution higher than 60% above 10 μg m^{-3} of PM_1. Organics were particularly important at high PM_1 levels, with their daytime concentrations overcoming 20 μg m^{-3} for levels above 25 μg m^{-3}. However, the contribution of eBC relatively to organics increased during evening for PM_1 levels above 25 μg m^{-3}, which was not significantly verified for PM_1 levels below this value. Interestingly, the daytime and evening eBC concentrations were also similar for PM_1 levels below 25 μg m^{-3} but the evening one increased sharply above that concentration. Therefore, eBC was particularly relevant during high pollution events, with biomass burning being likely a determinant source.

On the other hand, non-refractory inorganic constituents dominated PM_1 composition at concentrations below 5 μg m^{-3}, but their concentration was low for all PM_1 levels and their contribution decreased sharply above 5 μg m^{-3} of PM_1 because of the high increase in organics and eBC concentrations. Inorganic salt emissions are typically low in Finland and their increase in concentration is usually caused by long-range transport (Barreira et al., 2021; Niemi et al., 2009; Timonen et al., 2013).

3.1.3. Chemical composition of polycyclic aromatic compounds

At residential areas and town centre, PAHs were 6–10 times higher during evening comparatively to daytime (Fig. 3, black dots). This result suggests the important contribution of biomass burning to PAH emissions. The daytime PAH concentration at the industrial area was much larger than the ones at residential sites and town centre, but it was only slightly higher than the evening concentrations at the forementioned sites. On the other hand, the PAH concentration at the highway was significantly smaller, although the daytime concentration was similar to the ones measured at residential areas and town centre.

The concentration of PAH-related ions was evaluated to determine if the PAH composition was dependent on the sources. Even though non-PAH constituents with the same molecular formula may contribute to the concentration of PAH species (as referred in Sect. 2.3), the correlation between total PAHs obtained from UMR data and the sum of PAH-related ions showed a high correlation (R^2 = 0.87) and therefore the PAH-related ions were assumed to have a major contribution from PAHs. The most dominant PAH-related ion fragments at residential and town centre areas were $C_{10}H_8^+$ and $C_{18}H_{12}^+$, with an average evening concentration ranging between of 0.01–0.02 μg m^{-3}, followed by $C_{12}H_8^+$ compounds (average evening concentrations of about 0.01 μg m^{-3}). The remaining measured PAH-related ions ($C_{12}H_{10}^+$, $C_{13}H_{10}^+$ and $C_{14}H_{10}^+$) at the referred locations constituted all together an average evening concentration of about 0.01 μg m^{-3}.

Interestingly, the $C_{18}H_{12}^+$ concentration at the industrial area was higher than the ones measured at residential and town centre areas during evening, with an average concentration of 0.02 μg m^{-3}, while all other concentrations of PAH-related ions were lower. This ion also increased at the background site during daytime (average concentration of 0.01 μg m^{-3}). A possible explanation for these results could be related to a preferential production of these compounds by industrial activities as the site was mainly downwind the industrial area due to the northern wind. In fact, the coefficient of determination of this ion with BC_{WB} was low (R^2 = 0.39), contrary to what was observed for the remaining measured PAH-like ions (R^2 values ranging between 0.61 and 0.84) (Table S2). The differences in the relative contribution of PAH-related ions at the studied locations may be important since the PAH health effects are highly compound specific (da Silva Junior et al., 2021; e.g. Sahoo et al., 2020).

3.1.4. Chemical speciation of trace elements

The concentration of eight elements (K, Cl, Cr, Cu, Fe, Na, V, and Zn) in PM_1 was evaluated (Fig. 4). The highest total amount of these elements was observed at the background site in the evening and industrial

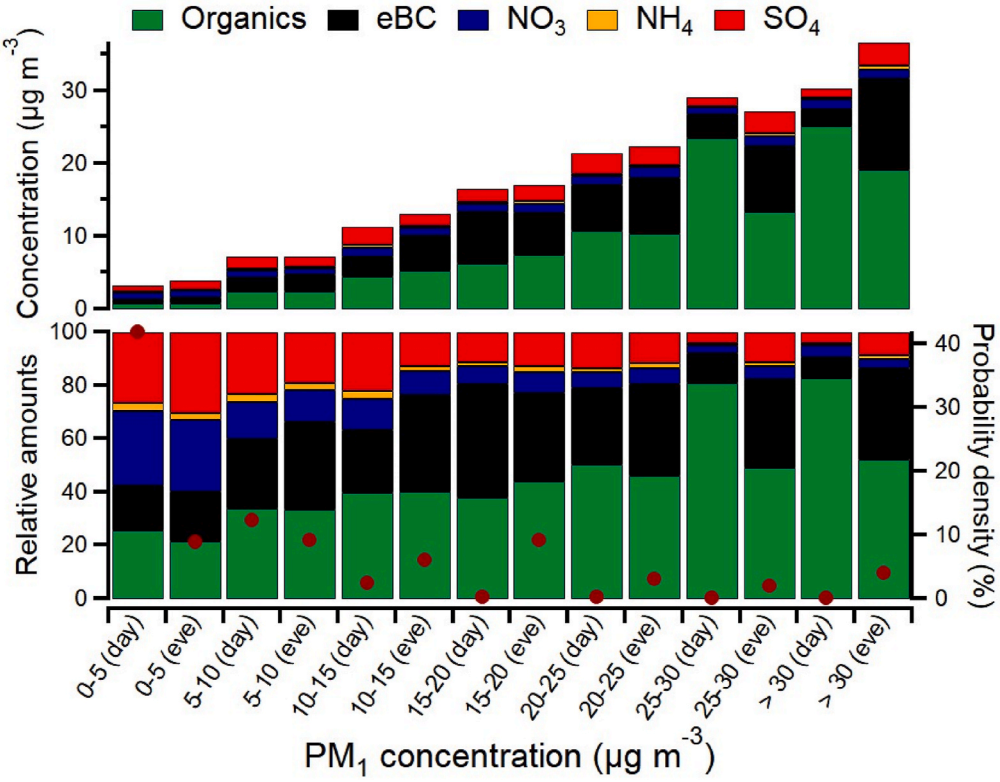

Fig. 2. Mean concentration and relative amounts of PM_1 species measured by the SP-AMS (organics, NO_3, NH_4, and SO_4) and by AE33 aethalometer (eBC) for different day and evening PM_1 concentration levels (sum of referred constituents).

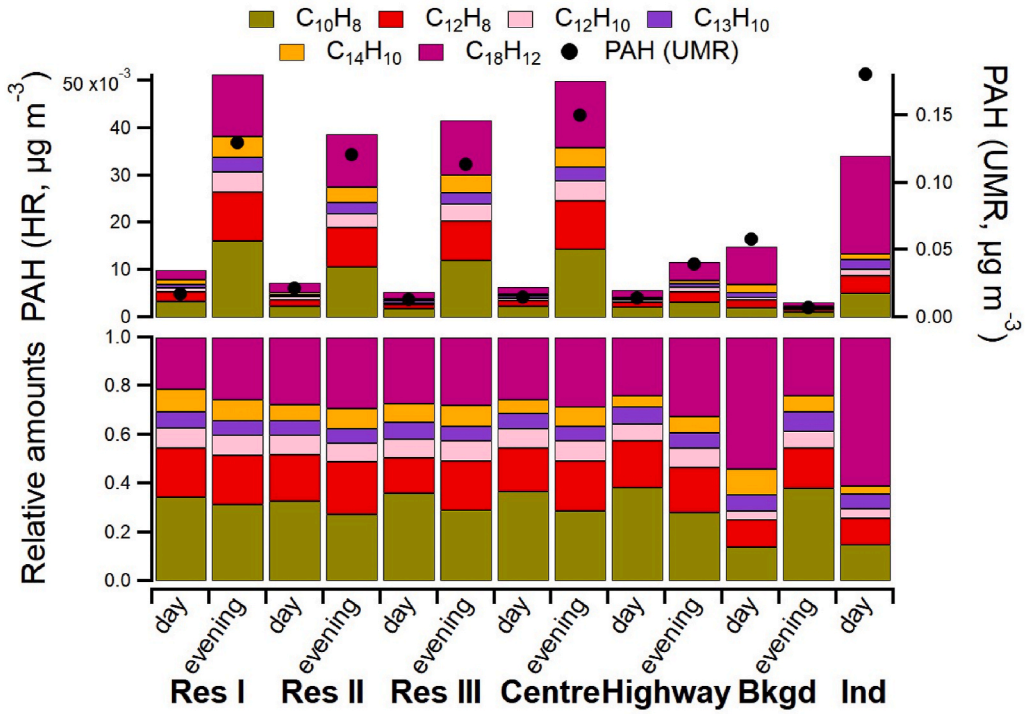

Fig. 3. Mean concentration and relative amounts of PAH-related ions ($C_{10}H_8^+$+$C_{12}H_8^+$+$C_{12}H_{10}^+$+$C_{13}H_{10}^+$+$C_{14}H_{10}^+$+$C_{18}H_{12}^+$) measured by the SP-AMS at residential areas (Res I-III), town centre, highway, background site (Bkgd), and industrial area (Ind) during day and evening. The total PAH concentration estimated using the method described in Dzepina et al. (2007) was also included.

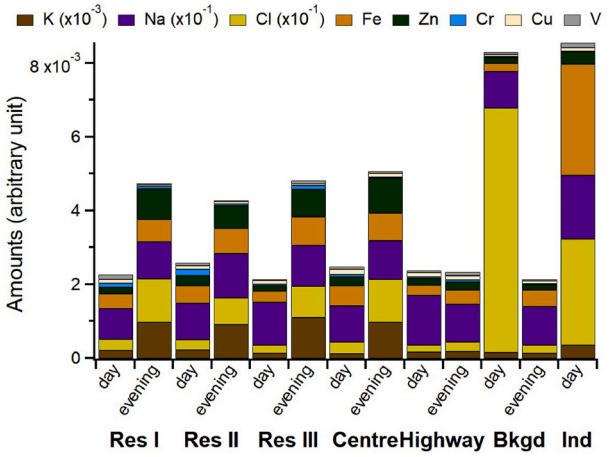

Fig. 4. Mean amounts of elements (K ($x10^{-3}$), Na ($x10^{-1}$), Cl ($x10^{-1}$), Fe, Zn, Cr, Cu, and V) measured by the SP-AMS at residential areas (Res I-III), town centre, highway, background site (Bkgd), and industrial area (Ind) during day and evening. Note that the amounts of elements presented in the figure are in arbitrary unit, and therefore the elements are not quantitatively comparable (see Sect. 2.3).

area, even though a significant increase was also observed at residential areas and town centre during evening. On the other hand, the total amount of elements at the highway was similar to the one at residential and town centre areas during daytime. Note, however, that the results of this study are semi-quantitative, and therefore a conversion of obtained signal into concentrations could change the total quantity of elements at the studied sites.

The amounts of potassium, chloride, and zinc were higher during evenings at residential areas and town centre (Fig. 4). Potassium (in particular its water-soluble fraction) is commonly used as a biomass burning tracer, in the absence of other significant sources of this element, and zinc has been previously shown to become enriched in the fine particle fraction during biomass combustion (Cheng et al., 2013; e.g. Uski et al., 2015). On the other hand, chloride is usually separated in two components, the sea-salt chloride and the non-sea-salt chloride, with the latest component being commonly emitted e.g. by waste incineration, coal combustion, biomass burning, and secondary organic aerosol formation (e.g. Sun et al., 2013; Yin et al., 2014; Zhao and Gao, 2008). Generally, sites with low particle pollution have higher correlation between sodium and chloride while this correlation decreases at sites with heavier particle pollution resulting in non-sea-salt chloride emissions (e.g. Yin et al., 2014), chiefly because most of fine sodium is derived from sea salt (e.g. Ooki et al., 2002). In our study, the amounts of sodium were relatively constant during day and evening, contrasting with what was observed for chloride and contributing to a poor correlation between these elements ($R^2 = 0.12$, Table S2). This finding suggests that chloride was mostly emitted by anthropogenic activities in our study. Furthermore, the amounts of sodium at the background site were similar to the ones at populated areas, which indicates that this element was likely originated from regional/long-range transport.

The amounts of chloride were the highest in the industrial area, where the amounts of iron also greatly increased. These results seem to indicate that industrial processes were an important source of these elements. Trace amounts of chromium, copper, and vanadium were also measured at all studied sites. Nonetheless, these elements did not show any significant changes between morning and evening, and therefore these components were likely not predominantly originated from biomass burning but instead from other sources such as industrial activities, fossil fuel combustion, or ship emissions (e.g. Fishbein, 1981; Rehman et al., 2019; Visschedijk et al., 2013).

High chloride amounts were also seen at the background site and were likely originated from the industrial emissions. However, those high concentrations were only observed on one campaign day (29th of January) when the wind direction was greatly favoring the transport of those emissions through the background site on the referred day

(Fig. S4). Characteristic particle size distributions from the industrial area (see Sect. 3.4) were also observed at the background site during the correspondent period of time.

3.2. Source apportionment of particulate organics and black carbon

The sources of OA were investigated using the PMF analysis (Fig. 5 and S6). As seen in Fig. S6, OA was divided into 4 factors: biomass burning OA (BBOA), hydrocarbon-like OA (HOA), semi-volatile oxygenated OA (SV-OOA), and low-volatility oxygenated OA (LV-OOA). The mass spectra of BBOA had clear m/z 60 ($C_2H_4O_2^+$) and m/z 73 ($C_3H_5O_2^+$) mass peaks, which have been used as tracers for biomass burning (Alfarra et al., 2007; e.g. Saarikoski et al., 2019). For BBOA, the oxygen-to-carbon (O/C) ratio was 0.4 and the hydrogen-to-carbon (H/C) ratio was 1.7. The mass spectra of HOA factor that is usually associated with traffic emissions (Zhang et al., 2005) was dominated by $C_XH_Y^+$ fragments, with the highest signal being obtained for m/z 57 ($C_4H_9^+$). Therefore, its O/C ratio was the lowest (0.07) and the H/C ratio the highest (2.2) of all factors. SV-OOA had a high signal at m/z 43 ($C_2H_3O^+$) and m/z 44 (CO_2^+). SV-OOA was more oxidized than BBOA, with O/C and H/C ratios of 0.6 and 1.7 respectively. LV-OOA had the largest signal at m/z 44 (CO_2^+) but, different from SV-OOA, was missing m/z 43 ($C_2H_3O^+$) almost totally. That was expected for aged particles. On the other hand, the O/C and H/C ratios of LV-OOA were smaller than those of SV-OOA being 0.4 and 1.3, respectively, which suggests a dominance of long-chain molecules on the LV-OOA spectra.

The average concentrations of the PMF factors and their relative contributions in OA are represented in Fig. 5. Primary organic aerosol factors, BBOA and HOA, had the highest concentrations during the measurement period, being particularly large during evenings. The BBOA evening concentration and contribution were the highest at Res I (3.85 μg m^{-3}, 51%), but elevated evening concentrations and contributions were also measured at other residential areas and town centre (average of 2.07–2.39 μg m^{-3}, 27–46%). HOA was clearly dominant at the town centre, with an evening concentration of 5.21 μg m^{-3} and the contribution of 59%. The increase in BBOA and HOA in the evening has also been reported in a recent study at an urban detached housing area located in Helsinki, Finland (Teinilä et al., 2022), the increase explained by both local emission sources and reduced mixing due to atmospheric inversion episodes.

The lowest concentrations were measured for oxygenated factors, SV-OOA and LV-OOA, with the maximum average values of 0.96 μg m^{-3} and 0.73 μg m^{-3}, respectively. The concentration of SV-OOA did not change significantly between day and evening being also similar in all measurement sites. Therefore, the SV-OOA was not likely to be predominantly originated from local sources. On the other hand, the LV-OOA concentration was slightly higher in residential and town centre areas during evening, which may have been at least partially caused by atmospheric accumulation and processing of local emissions.

Concerning the source apportionment for BC, the concentrations of BC_{FF} and BC_{WB} broadly followed those obtained for HOA and BBOA, respectively (Fig. 5) with both BC_{FF} and BC_{WB} being higher during evening at residential sites and town centre. The contributions of BC_{FF} and BC_{WB} were relatively similar at most of the sites, with an exception for Res II where the BC_{WB} contribution was clearly higher and highway where BC_{FF} was larger than BC_{WB}. These results seem to indicate that both BC from traffic and biomass burning constitute important pollutants during winter evenings.

The high biomass burning emissions of OA and eBC at the town centre contrasted with what has been commonly observed at more populated cities in northern Europe where wood burning for heating purposes has been drastically reduced in the past decades and BBOA fraction is often challenging to obtain since most of wood burning occurs in suburban areas (Aurela et al., 2015; Barreira et al., 2021; Saarikoski

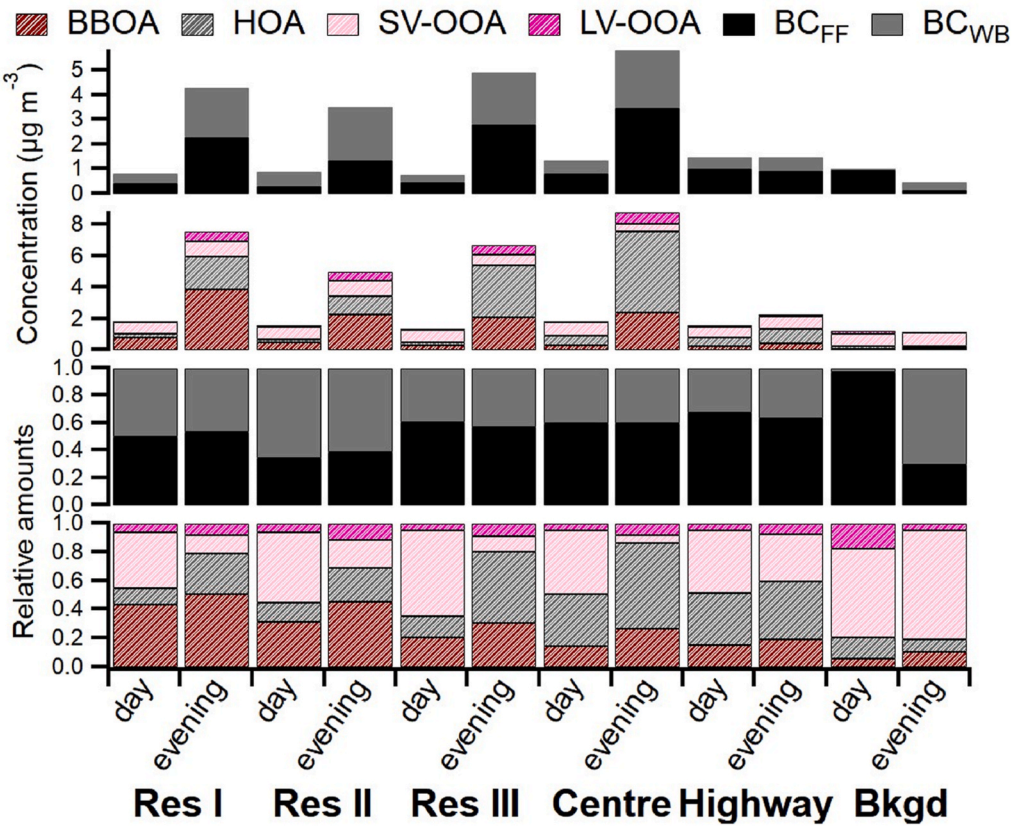

Fig. 5. Source apportionment of OA by Positive Matrix Factorization and of eBC using the aethalometer model at residential areas (Res I-III), town centre, highway (HWY), and background site (Bkgd) during day and evening.

et al., 2021). The high contribution of emissions from biomass burning may therefore be characteristic for small towns in northern latitudes, where a significant share of residences uses biomass burning in the centre of the town. In fact, a study involving aerosol measurements of elemental carbon (EC) and organic carbon (OC) at several background sites in northern Europe identified biomass burning as the major source of OC at all sites during winter (Glasius et al., 2018). However, it is likely an issue that is transversal to many residential areas around the globe. For example, a study performed by Liakakou et al. (2020) in Athens, Greece, showed that wood burning can contribute as much as fossil fuels to PM during winter evenings; and Quinteros et al. (2023) and Reyes et al. (2021) found high concentrations of levoglucosan (wood burning tracer) at the city of Temuco, Chile. A modelling study on sources of OA in Europe has also identified wood burning as the dominant source in winter, constituting about 61% of total OA (Jiang et al., 2019). This issue may become even more important in future years due to rising energy prices, which may lead to an increase in the usage of wood burners as they provide cheap and reliable energy.

3.3. Particle size distributions and respiratory tract deposition

Particle number and LDSA size distributions were also evaluated for the studied sites. In terms of number size distributions, the contribution of particles larger than approx. 50 nm increased during evenings at Res I-III and town centre (Fig. 6). The increase of that size particles can be linked with the biomass combustion (e.g. Lepistö et al., 2023). The concentration of particles smaller than 50 nm increased also during evenings in Res III and town centre, which indicates a larger contribution from traffic (Barreira et al., 2021; e.g. Ondráček et al., 2011; Rönkkö et al., 2017). The increase in particle concentration at Res III for sizes below 50 nm is likely explained by the fact that this site is located near the town centre. In the highway, the concentration of particles smaller than 50 nm was relatively high during daytime suggesting a clear contribution from traffic, whereas in the evening number concentration was smaller. Also, the concentration of particles larger than 50 nm was low in the highway, showing that the effects of evening-time biomass combustion was not observed in the highway. In the background site, both daytime and evening number size distributions peaked between the sizes of 20 and 50 nm, which is not typical for the regional background aerosol in Finland. This size range also does not correspond well with the size distributions from traffic nor biomass combustion. In addition, the concentration levels were not dependent on the time of the day. Therefore, it is likely that the industrial area has affected the particle number concentrations in the background site even though these increased concentrations were not as clearly observed for PM_1 mass.

The increased particle emissions from biomass burning during the evenings corresponded as well to an increase in LDSA. The contribution of biomass combustion to LDSA was seen in the size range of 50–400 nm, being in agreement with the previous measurements at residential areas such as in e.g. Teinilä et al. (2022) and Lepistö et al. (2023). On the other hand, in the highway, LDSA was dominated by particles smaller than 100 nm, which is typical for traffic locations (e.g., Lepistö et al. (2022)). The fraction of sub 100 nm particles was seen as well for LDSA in the town centre, supporting the role of traffic. In the background site, increased LDSA concentrations were observed for particles of around 50–100 nm, which also differs from typical background LDSA size distributions at regional background sites in Finland (e.g. Lepistö et al., 2023; Salo et al., 2021; Teinilä et al., 2022). The average daytime LDSA concentrations (Table S3) were 12.5–17.6, 24.1, 29.0, and 18.4 $\mu m^2 m^{-3}$ in Res I-III, town centre, highway and background site, respectively. The average LDSA concentrations during the evenings were 30.5–41.6, 60.7, 24.7, and 16.9 $\mu m^2 m^{-3}$ in Res I-III, town centre, highway and background site, respectively. Thus, LDSA were 1.8–3.3 times higher during the evenings in the residential areas and town centre, whereas in the highway and background site there were not significant changes between day and evening concentrations. Also, it should be noted that the evening time LDSA concentrations in this study clearly exceeded typical LDSA concentrations (13.2–37.2 $\mu m^2 m^{-3}$) measured in the city centre of Helsinki (Kuula et al., 2020; Lepistö et al., 2022, 2023). These results emphasize the potential role of local sources of ultrafine particles on human health and the high relevance of these parameters in air quality studies and monitoring.

The particle size distributions and LDSA were also measured at the industrial area. As observed in Fig. 7, the number size distributions were dominated by ultrafine particles smaller than 100 nm, whereas LDSA size distribution peaked around 50–100 nm. Even though these size ranges were rather similar to the ones observed for traffic emissions (see e.g., the particle number size distributions at the highway during daytime in Fig. 6), the number size distribution at the industrial area was broader than the traffic one. Furthermore, an increase of particles up to 1 μm was observed in LDSA size distributions. These findings indicate the contribution of industrial processes in addition to heavy traffic inside the industrial area to number and LDSA size distributions. Also, both number and LDSA size distributions measured inside the industrial area were rather similar to the ones measured in the background site, supporting the role of industrial processes in PM measured at the

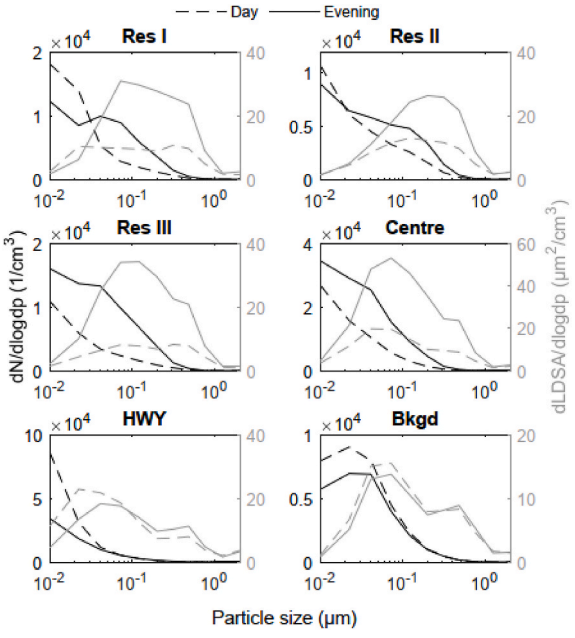

Fig. 6. Average particle number and LDSA size distributions at residential areas (Res I-III), town centre, highway, and background site (Bkgd) during day and evening. Note varying Y-axis scales.

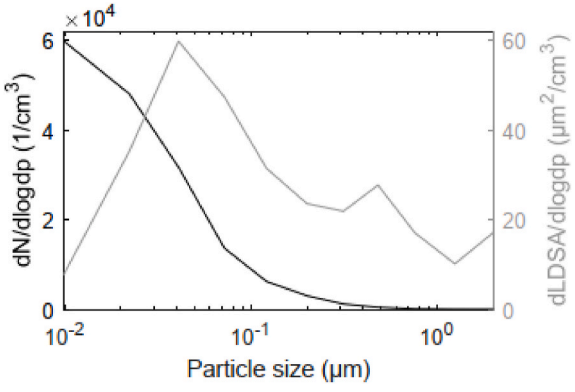

Fig. 7. Average particle number and LDSA size distributions measured inside the industrial area.

background site. The average LDSA concentration in the industrial area was 67.8 $\mu m^2 m^{-3}$, which exceeded the average daytime and evening time concentrations measured outside the industrial area and e.g., the typical LDSA concentrations in Helsinki city centre (13.2–37.2 $\mu m^2 m^{-3}$ (Kuula et al., 2020; Lepistö et al., 2023, 2022),).

The LDSA concentrations in Res I-III and town centre were clearly increased during the southern winds, especially for sizes between 50 and 200 nm, whereas in the background site the LDSA contribution for particles of this size range were higher during the northern winds (Fig. 8). During daytime, LDSA concentrations in Res I-III and town centre (Table S4) were 10.1–21.4 and 31.5–44.4 $\mu m^2 cm^{-3}$ with northern and southern winds, respectively. On evenings, LDSA concentrations were 22.5–35.5 and 39.7–107.4 $\mu m^2 cm^{-3}$, respectively. Thus, southern winds clearly affected the LDSA concentrations in residential areas and town centre. The fact that increased LDSA concentrations were also observed during daytime suggests a larger role of industrial emissions compared to biomass combustion. These increases were observed for particle number size distributions as well (Fig. S7). However, the concentration increase with LDSA was seen for a wide size range (50 nm–500 nm) (Fig. 8), which does not correspond totally with the number size distributions measured inside the industrial area (Fig. 7). Also, the increased concentrations were observed in the highway as well, which is east from the industrial area. Thus, the cold temperatures and low wind speed had likely a significant effect in the increased concentrations during these southern wind periods in addition to the industrial emissions. However, during the northern wind periods, the increase in the particle number and LDSA (northern wind: 18.4–18.6 $\mu m^2 cm^{-3}$, southern wind: 12.3 $\mu m^2 cm^{-3}$) was clear in the background site, which shows that the industrial area influenced these parameters in nearby areas. Similar results have been found e.g., next to an airport (Lepistö et al., 2023). These observations emphasize the importance to understand the local ultrafine particle emission sources as they may have health effect despite not easily detected with typical mass-based measurements.

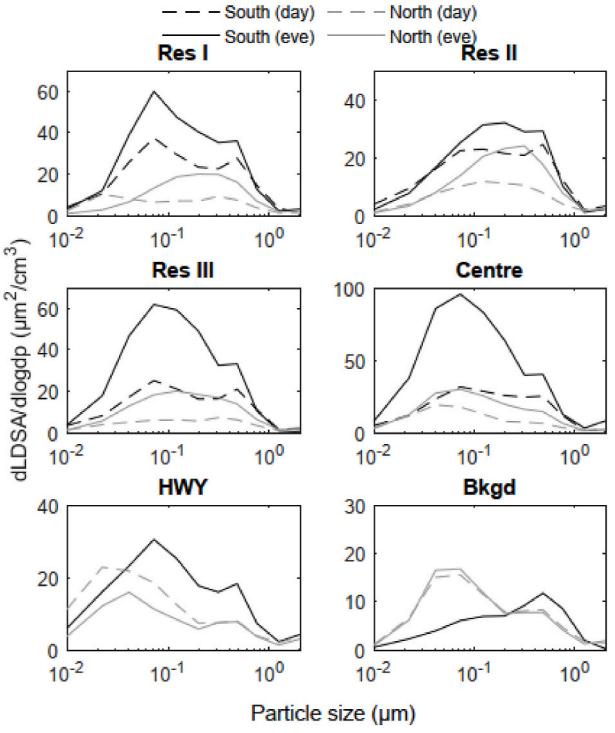

Fig. 8. LDSA size distributions at Res I (Lapaluoto), Res II (Varvi), Res III (Velkaperä), town centre, highway (HWY), and background site (Bkgd) on daily periods (day and evening) with southern and northern winds. Note varying Y-axis limits.

4. Conclusions

In this study, the sources and chemical and physical properties of PM_1 were evaluated at different sites (residential areas, town centre, highway, background site, and industrial area) of a small town located in northern Finland. A mobile laboratory containing a wide setup of advanced research instruments was used for that purpose, which enabled to investigate the spatial and temporal variation of PM_1 properties and sources in a matter of few days and, therefore, to provide new information on the air quality of a Nordic small town as well as the origin of atmospheric pollutants. The results showed clearly that biomass burning was a major source of PM_1 constituents in inhabited areas, especially during evenings. In particular, a significant increase in organics (including PAHs) and eBC from biomass burning was found in these areas. However, traffic was also a significant source of organics and eBC. Characteristic particle number and LDSA size distributions from biomass burning and traffic were also observed at the mentioned areas. The high contribution from biomass burning may be characteristic for small towns in northern latitudes due to a high share of residences using this type of energy for heating purposes. However, the fraction of biomass burning emissions may rise generally in future years due to increasing energy costs, which may lead to an intensification of wood burning, and to the electrification of car fleet. The intensification of wood combustion would likely have implications on air quality, especially when considering that some constituents of biomass burning aerosols, such as black carbon and PAHs, have been associated with adverse health effects.

In addition to biomass burning and traffic, emissions from a relatively large industrial area located in the southwest from the town centre had an impact on PM chemical composition, number concentrations and LDSA. A clear increase in several PM_1 constituents (sulfate, eBC, organics, $C_{18}H_{12}^+$, Cl, and Fe) was observed at the industrial area, even though that increase seemed to be more intermittent than at the other measured locations. Characteristic particle number and LDSA size distributions from industrial emissions were also identified. The effect of industrial emissions on inhabited areas was more evident in particle number concentrations and LDSA than in particulate mass and chemical composition.

The results from this study reinforce the importance of implementing additional metrics to evaluate atmospheric pollution and its effect on air quality since e.g. $PM_{2.5}$ levels recommended by WHO do not take into account the size of the particles. The monitoring of particle number has been recently introduced on the WHO air quality guidelines as a good practice statement. Nonetheless, guideline levels for particle number concentration were still not formulated. A possible metric that could be as well implemented is LDSA since it helps to differentiate the effect of different sources on particulate alveolar deposition. The chemical composition of PM should be also considered in future metrics of atmospheric pollution since its link with health effects are widely recognized. In fact, there is no current evidence of safe levels of PM exposure or a threshold below which no adverse health effects would occur due to the role of chemical composition. The understanding of the dynamics of atmospheric composition and of its spatiotemporally, as shown also in this study, will likely be of key importance to develop metrics that can more accurately represent the potential health effects of inhaling and ingesting the enormous diversity of chemicals that are present in anthropogenic aerosols.

Credit author statement

Luis M.F. Barreira: Data curation, Formal analysis, Investigation, Methodology, Software, Validation, Visualization, Roles/Writing - original draft, and Writing - review & editing; Teemu Lepistö: Conceptualization, Data curation, Formal analysis, Investigation, Methodology, Software, Validation, Visualization, Roles/Writing - original draft, and Writing - review & editing; Laura Salo and Aku Helin: Investigation,

Methodology, and Writing - review & editing; Minna Aurela and Niina Kuittinen: Methodology, and Writing - review & editing; Sanna Saarikoski, Topi Rönkkö, and Hilkka Timonen: Conceptualization, Funding acquisition, Methodology, Project administration, Resources, Supervision, Validation, and Writing - review & editing.

Declaration of competing interest

The authors declare that they have no known competing financial interests or personal relationships that could have appeared to influence the work reported in this paper.

Acknowledgements

This work was supported by the Black Carbon Footprint project, funded by Business Finland (grant 528/31/2019) and participating companies, the European Commission, Horizon 2020 framework program (TUBE; grant no. 814978) and the ACCC Flagship funded by the Academy of Finland (grant nos. 337551 and 337552). The city of Raahe is also acknowledged for their help in air quality measurements.

Appendix A. Supplementary data

Supplementary data to this article can be found online at https://doi.org/10.1016/j.apr.2023.101835.

References

Aguilera, I., Dratva, J., Caviezel, S., Burdet, L., de, G.E., Ducret-Stich, R.E., Eeftens, M., Keidel, D., Meier, R., Perez, L., Rothe, T., Schaffner, E., Schmit-Trucksäss, A., Tsai, M.-Y., Schindler, C., Künzli, N., Probst-Hensch, N., 2016. Particulate matter and subclinical atherosclerosis: associations between different particle sizes and sources with carotid intima-media thickness in the SAPALDIA study. Environ. Health Perspect. 124, 1700–1706. https://doi.org/10.1289/EHP161.

Alfarra, M.R., Prevot, A.S.H., Szidat, S., Sandradewi, J., Weimer, S., Lanz, V.A., Schreiber, D., Mohr, M., Baltensperger, U., 2007. Identification of the mass spectral signature of organic aerosols from wood burning emissions. Environ. Sci. Technol. 41, 5770–5777. https://doi.org/10.1021/es062289b.

Aurela, M., Saarikoski, S., Niemi, J.V., Canonaco, F., Prevot, A.S.H., Frey, A., Carbone, S., Kousa, A., Hillamo, R., 2015. Chemical and source characterization of submicron particles at residential and traffic sites in the Helsinki metropolitan area, Finland. Aerosol Air Qual. Res. 15, 1213–1226. https://doi.org/10.4209/aaqr.2014.11.0279.

Barreira, L.M.F., Helin, A., Aurela, M., Teinilä, K., Friman, M., Kangas, L., Niemi, J.V., Portin, H., Kousa, A., Pirjola, L., Rönkkö, T., Saarikoski, S., Timonen, H., 2021. In-depth characterization of submicron particulate matter inter-annual variations at a street canyon site in northern Europe. Atmos. Chem. Phys. 21, 6297–6314. https://doi.org/10.5194/acp-21-6297-2021.

Brauer, M., Casadei, B., Harrington, R.A., Kovacs, R., Sliwa, K., 2021. Taking a stand against air pollution—the impact on cardiovascular disease. Circulation 143, e800. https://doi.org/10.1161/CIRCULATIONAHA.120.052666. –e804.

Canagaratna, M.R., Jayne, J.T., Jimenez, J.L., Allan, J.D., Alfarra, M.R., Zhang, Q., Onasch, T.B., Drewnick, F., Coe, H., Middlebrook, A., Delia, A., Williams, L.R., Trimborn, A.M., Northway, M.J., DeCarlo, P.F., Kolb, C.E., Davidovits, P., Worsnop, D.R., 2007. Chemical and microphysical characterization of ambient aerosols with the aerodyne aerosol mass spectrometer. Mass Spectrom. Rev. 26, 185–222. https://doi.org/10.1002/mas.20115.

Carbone, S., Onasch, T., Saarikoski, S., Timonen, H., Saarnio, K., Sueper, D., Rönkkö, T., Pirjola, L., Häyrinen, A., Worsnop, D., Hillamo, R., 2015. Characterization of trace metals on soot aerosol particles with the SP-AMS: detection and quantification. Atmos. Meas. Tech. 8, 4803–4815. https://doi.org/10.5194/amt-8-4803-2015.

Chan, C.K., Yao, X., 2008. Air pollution in mega cities in China. Atmos. Environ. 42, 1–42. https://doi.org/10.1016/j.atmosenv.2007.09.003.

Chen, G., Canonaco, F., Tobler, A., Aas, W., Alastuey, A., Allan, J., Atabakhsh, S., Aurela, M., Baltensperger, U., Bougiatioti, A., De Brito, J.F., Ceburnis, D., Chazeau, B., Chebaicheb, H., Daellenbach, K.R., Ehn, M., El Haddad, I., Eleftheriadis, K., Favez, O., Flentje, H., Font, A., Fossum, K., Freney, E., Gini, M., Green, D.C., Heikkinen, L., Herrmann, H., Kalogridis, A.-C., Keernik, H., Lhotka, R., Lin, C., Lunder, C., Maasikmets, M., Manousakas, M.I., Marchand, N., Marin, C., Marmureanu, L., Mihalopoulos, N., Močnik, G., Nęcki, J., O'Dowd, C., Ovadnevaite, J., Peter, T., Petit, J.-E., Pikridas, M., Matthew Platt, S., Pokorná, P., Poulain, L., Priestman, M., Riffault, V., Rinaldi, M., Różański, K., Schwarz, J., Sciare, J., Simon, L., Skiba, A., Slowik, J.G., Sosedova, Y., Stavroulas, I., Styszko, K., Teinemaa, E., Timonen, H., Tremper, A., Vasilescu, J., Via, M., Vodička, P., Wiedensohler, A., Zografou, O., Cruz Minguillón, M., Prévôt, A.S.H., 2022. European aerosol phenomenology – 8: harmonised source apportionment of organic aerosol using 22 Year-long ACSM/AMS datasets. Environ. Int. 166, 107325 https://doi.org/10.1016/j.envint.2022.107325.

Cheng, Y., Engling, G., He, K.-B., Duan, F.-K., Ma, Y.-L., Du, Z.-Y., Liu, J.-M., Zheng, M., Weber, R.J., 2013. Biomass burning contribution to Beijing aerosol. Atmos. Chem. Phys. 13, 7765–7781. https://doi.org/10.5194/acp-13-7765-2013.

da Silva Junior, F.C., Felipe, M.B.M.C., Castro, D.E.F. de, Araújo, S.C., da, S., Sisenando, H.C.N., Batistuzzo de Medeiros, S.R., 2021. A look beyond the priority: a systematic review of the genotoxic, mutagenic, and carcinogenic endpoints of non-priority PAHs. Environ. Pollut. 278, 116838 https://doi.org/10.1016/j.envpol.2021.116838.

Dall'Osto, M., Drewnick, F., Fisher, R., Harrison, R.M., 2012. Real-time measurements of nonmetallic fine particulate matter adjacent to a major integrated steelworks. Aerosol Sci. Technol. 46, 639–653. https://doi.org/10.1080/02786826.2011.647120.

Drinovec, L., Močnik, G., Zotter, P., Prévôt, A.S.H., Ruckstuhl, C., Coz, E., Rupakheti, M., Sciare, J., Müller, T., Wiedensohler, A., Hansen, A.D.A., 2015. The "dual-spot" Aethalometer: an improved measurement of aerosol black carbon with real-time loading compensation. Atmos. Meas. Tech. 8, 1965–1979. https://doi.org/10.5194/amt-8-1965-2015.

Dzepina, K., Arey, J., Marr, L.C., Worsnop, D.R., Salcedo, D., Zhang, Q., Onasch, T.B., Molina, L.T., Molina, M.J., Jimenez, J.L., 2007. Detection of particle-phase polycyclic aromatic hydrocarbons in Mexico City using an aerosol mass spectrometer. Int. J. Mass Spectrom. 263, 152–170. https://doi.org/10.1016/j.ijms.2007.01.010.

Fishbein, L., 1981. Sources, transport and alterations of metal compounds: an overview. I. Arsenic, beryllium, cadmium, chromium, and nickel. Environ. Health Perspect. 40, 43–64. https://doi.org/10.1289/ehp.814043.

Glasius, M., Hansen, A.M.K., Claeys, M., Henzing, J.S., Jedynska, A.D., Kasper-Giebl, A., Kistler, M., Kristensen, K., Martinsson, J., Maenhaut, W., Nøjgaard, J.K., Spindler, G., Stenström, K.E., Swietlicki, E., Szidat, S., Simpson, D., Yttri, K.E., 2018. Composition and sources of carbonaceous aerosols in Northern Europe during winter. Atmos. Environ. 173, 127–141. https://doi.org/10.1016/j.atmosenv.2017.11.005.

Hakkarainen, H., Salo, L., Mikkonen, S., Saarikoski, S., Aurela, M., Teinilä, K., Ihalainen, M., Martikainen, S., Marjanen, P., Lepistö, T., Kuittinen, N., Saarnio, K., Aakko-Saksa, P., Pfeiffer, T.V., Timonen, H., Rönkkö, T., Jalava, P.I., 2022. Black carbon toxicity dependence on particle coating: measurements with a novel cell exposure method. Sci. Total Environ. 838, 156543 https://doi.org/10.1016/j.scitotenv.2022.156543.

Herring, C.L., Faiola, C.L., Massoli, P., Sueper, D., Erickson, M.H., McDonald, J.D., Simpson, C.D., Yost, M.G., Jobson, B.T., VanReken, T.M., 2015. New methodology for quantifying polycyclic aromatic hydrocarbons (PAHs) using high-resolution aerosol mass spectrometry. Aerosol Sci. Technol. 49, 1131–1148. https://doi.org/10.1080/02786826.2015.1101050.

Heusinkveld, H.J., Wahle, T., Campbell, A., Westerink, R.H.S., Tran, L., Johnston, H., Stone, V., Cassee, F.R., Schins, R.P.F., 2016. Neurodegenerative and neurological disorders by small inhaled particles. Neurotoxicology 56, 94–106. https://doi.org/10.1016/j.neuro.2016.07.007.

Hinds, W.C., Zhu, Y., 1999. Aerosol Technology: Properties, Behavior, and Measurement of Airborne Particles. JohnWiley & Sons Inc, New York.

ICRP, 1994. Human Respiratory Tract Model for Radiological Protection. ICRP Publication 66. Ann. ICRP 24 (1-3).

Järvinen, A., Aitomaa, M., Rostedt, A., Keskinen, J., Yli-Ojanperä, J., 2014. Calibration of the new electrical low pressure impactor (ELPI+). J. Aerosol Sci. 69, 150–159. https://doi.org/10.1016/j.jaerosci.2013.12.006.

Jiang, J., Aksoyoglu, S., El-Haddad, I., Ciarelli, G., Denier van der Gon, H.A.C., Canonaco, F., Gilardoni, S., Paglione, M., Minguillón, M.C., Favez, O., Zhang, Y., Marchand, N., Hao, L., Virtanen, A., Florou, K., O'Dowd, C., Ovadnevaite, J., Baltensperger, U., Prévôt, A.S.H., 2019. Sources of organic aerosols in Europe: a modeling study using CAMx with modified volatility basis set scheme. Atmos. Chem. Phys. 19, 15247–15270. https://doi.org/10.5194/acp-19-15247-2019.

Jimenez, J.L., Jayne, J.T., Shi, Q., Kolb, C.E., Worsnop, D.R., Yourshaw, I., Seinfeld, J.H., Flagan, R.C., Zhang, X., Smith, K.A., Morris, J.W., Davidovits, P., 2003. Ambient aerosol sampling using the aerodyne aerosol mass spectrometer. J. Geophys. Res. Atmos. 108, 1–13. https://doi.org/10.1029/2001JD001213.

Karjalainen, P., Rönkkö, T., Simonen, P., Ntziachristos, L., Juuti, P., Timonen, H., Teinilä, K., Saarikoski, S., Saveljeff, H., Lauren, M., Happonen, M., Matilainen, P., Maunula, T., Nuottimäki, J., Keskinen, J., 2019. Strategies to diminish the emissions of particles and secondary aerosol formation from diesel engines. Environ. Sci. Technol. 53, 10408–10416. https://doi.org/10.1021/acs.est.9b04073.

Keskinen, J., Pietarinen, K., Lehtimäki, M., 1992. Electrical low pressure impactor. J. Aerosol Sci. 23, 353–360. https://doi.org/10.1016/0021-8502(92)90004-F.

Kuula, J., Kuuluvainen, H., Niemi, J.V., Saukko, E., Portin, H., Kousa, A., Aurela, M., Rönkkö, T., Timonen, H., 2020. Long-term sensor measurements of lung deposited surface area of particulate matter emitted from local vehicular and residential wood combustion sources. Aerosol Sci. Technol. 54, 190–202. https://doi.org/10.1080/02786826.2019.1668909.

Lee, J.Y., Daube, C., Fortner, E., Ellsworth, N., May, N.W., Tallant, J., Herndon, S., Pratt, K.A., 2023. Chemical characterization of prescribed burn emissions from a mixed forest in Northern Michigan. Environ. Sci.: Atmosphere 3, 35–48. https://doi.org/10.1039/D2EA00069E.

Lepistö, T., Barreira, L.M.F., Helin, A., Niemi, J.V., Kuittinen, N., Lintusaari, H., Silvonen, V., Markkula, L., Manninen, H.E., Timonen, H., Jalava, P., Saarikoski, S., Rönkkö, T., 2023. Snapshots of wintertime urban aerosol characteristics: local sources emphasized in ultrafine particle number and lung deposited surface area. Environ. Res. 231, 116068 https://doi.org/10.1016/j.envres.2023.116068.

Lepistö, T., Kuuluvainen, H., Juuti, P., Järvinen, A., Arffman, A., Rönkkö, T., 2020. Measurement of the human respiratory tract deposited surface area of particles with

an electrical low pressure impactor. Aerosol Sci. Technol. 54, 958–971. https://doi.org/10.1080/02786826.2020.1745141.
Lepistö, T., Kuuluvainen, H., Lintusaari, H., Kuittinen, N., Salo, L., Helin, A., Niemi, J.V., Manninen, H.E., Timonen, H., Jalava, P., Saarikoski, S., Rönkkö, T., 2022. Connection between lung deposited surface area (LDSA) and black carbon (BC) concentrations in road traffic and harbour environments. Atmos. Environ. 272, 118931 https://doi.org/10.1016/j.atmosenv.2021.118931.
Liakakou, E., Kaskaoutis, D.G., Grivas, G., Stavroulas, I., Tsagkaraki, M., Paraskevopoulou, D., Bougiatioti, A., Dumka, U.C., Gerasopoulos, E., Mihalopoulos, N., 2020. Long-term brown carbon spectral characteristics in a Mediterranean city (Athens). Sci. Total Environ. 708, 135019 https://doi.org/10.1016/j.scitotenv.2019.135019.
Middlebrook, A.M., Bahreini, R., Jimenez, J.L., Canagaratna, M.R., 2012. Evaluation of composition-dependent collection efficiencies for the aerodyne aerosol mass spectrometer using field data. Aerosol Sci. Technol. 46, 258–271. https://doi.org/10.1080/02786826.2011.620041.
Niemi, J.V., Saarikoski, S., Aurela, M., Tervahattu, H., Hillamo, R., Westphal, D.L., Aarnio, P., Koskentalo, T., Makkonen, U., Vehkamäki, H., Kulmala, M., 2009. Long-range transport episodes of fine particles in southern Finland during 1999–2007. Atmos. Environ. 43, 1255–1264. https://doi.org/10.1016/j.atmosenv.2008.11.022.
Ohlwein, S., Kappeler, R., Kutlar Joss, M., Künzli, N., Hoffmann, B., 2019. Health effects of ultrafine particles: a systematic literature review update of epidemiological evidence. Int. J. Publ. Health 64, 547–559. https://doi.org/10.1007/s00038-019-01202-7.
Onasch, T.B., Trimborn, A., Fortner, E.C., Jayne, J.T., Kok, G.L., Williams, L.R., Davidovits, P., Worsnop, D.R., 2012. Soot particle aerosol mass spectrometer: development, validation, and initial application. Aerosol Sci. Technol. 46, 804–817. https://doi.org/10.1080/02786826.2012.663948.
Ondráček, J., Schwarz, J., Ždímal, V., Andělová, L., Vodička, P., Bízek, V., Tsai, C.-J., Chen, S.-C., Smolík, J., 2011. Contribution of the road traffic to air pollution in the Prague city (busy speedway and suburban crossroads). Atmos. Environ. 45, 5090–5100. https://doi.org/10.1016/j.atmosenv.2011.06.036.
Ooki, A., Uematsu, M., Miura, K., Nakae, S., 2002. Sources of sodium in atmospheric fine particles. Atmos. Environ. 36, 4367–4374. https://doi.org/10.1016/S1352-2310(02)00341-2.
Pan, S., Qiu, Y., Li, M., Yang, Z., Liang, D., 2022. Recent developments in the determination of PM2.5 chemical composition. Bull. Environ. Contam. Toxicol. 108, 819–823. https://doi.org/10.1007/s00128-022-03510-w.
Patel, S., Leavey, A., Sheshadri, A., Kumar, P., Kandikuppa, S., Tarsi, J., Mukhopadhyay, K., Johnson, P., Balakrishnan, K., Schechtman, K.B., Castro, M., Yadama, G., Biswas, P., 2018. Associations between household air pollution and reduced lung function in women and children in rural southern India. J. Appl. Toxicol. 38, 1405–1415. https://doi.org/10.1002/jat.3659.
Quinteros, M.E., Blanco, E., Sanabria, J., Rosas-Diaz, F., Blazquez, C.A., Ayala, S., Cárdenas-R, J.P., Stone, E.A., Sybesma, K., Delgado-Saborit, J.M., Harrison, R.M., Ruiz-Rudolph, P., 2023. Spatio-temporal distribution of particulate matter and wood-smoke tracers in Temuco, Chile: a city heavily impacted by residential wood-burning. Atmos. Environ. 294, 119529 https://doi.org/10.1016/j.atmosenv.2022.119529.
Rehman, M., Lijun, L., Wang, Q., Hamzah Saleem, M., Bashir, S., Baloch, S., Peng, D., 2019. Copper environmental toxicology, recent advances, and future outlook: a review. Environ. Sci. Pollut. Res. 26, 180016 https://doi.org/10.1007/s11356-019-05073-6.
Reyes, F., Ahumada, S., Rojas, F., Oyola, P., Vásquez, Y., Aguilera, C., Henriquez, A., Gramsch, E., Kang, C.-M., Saarikoski, S., Teinilä, K., Aurela, M., Timonen, H., 2021. Impact of biomass burning on air quality in Temuco city, Chile. Aerosol Air Qual. Res. 21, 210110 https://doi.org/10.4209/aaqr.210110.
Rönkkö, T., Kuuluvainen, H., Karjalainen, P., Keskinen, J., Hillamo, R., Niemi, J.V., Pirjola, L., Timonen, H.J., Saarikoski, S., Saukko, E., Järvinen, A., Silvennoinen, H., Rostedt, A., Olin, M., Yli-Ojanperä, J., Nousiainen, P., Kousa, A., Maso, M.D., 2017. Traffic is a major source of atmospheric nanocluster aerosol. Proc. Natl. Acad. Sci. USA 114, 7549–7554. https://doi.org/10.1073/pnas.1700830114.
Saarikoski, S., Niemi, J.V., Aurela, M., Pirjola, L., Kousa, A., Rönkkö, T., Timonen, H., 2021. Sources of black carbon at residential and traffic environments obtained by two source apportionment methods. Atmos. Chem. Phys. 21, 14851–14869. https://doi.org/10.5194/acp-21-14851-2021.
Saarikoski, S., Reyes, F., Vázquez, Y., Tagle, M., Timonen, H., Aurela, M., Carbone, S., Worsnop, D.R., Hillamo, R., Oyola, P., 2019. Characterization of submicron aerosol chemical composition and sources in the coastal area of Central Chile. Atmos. Environ. 199, 391–401. https://doi.org/10.1016/j.atmosenv.2018.11.040.
Sahoo, B.M., Kumar, B.V.V.R., Banik, B.K., Borah, P., 2020. Polyaromatic hydrocarbons (PAHs): structures, synthesis and their biological profile. Curr. Org. Synth. 17, 625–640. https://doi.org/10.2174/1570179417666200713182441.
Salcedo, D., Laskin, A., Shutthanandan, V., Jimenez, J.-L., 2012. Feasibility of the Detection of Trace Elements in Particulate Matter Using Online High-Resolution Aerosol Mass Spectrometry. Aerosol Sci. Technol. 46, 1187–1200. https://doi.org/10.1080/02786826.2012.701354.
Salo, L., Hyvärinen, A., Jalava, P., Teinilä, K., Hooda, R.K., Datta, A., Saarikoski, S., Lintusaari, H., Lepistö, T., Martikainen, S., Rostedt, A., Sharma, V.P., Rahman, MdH., Subudhi, S., Asmi, E., Niemi, J.V., Lihavainen, H., Lal, B., Keskinen, J., Kuuluvainen, H., Timonen, H., Rönkkö, T., 2021. The characteristics and size of lung-depositing particles vary significantly between high and low pollution traffic environments. Atmos. Environ. 255, 118421 https://doi.org/10.1016/j.atmosenv.2021.118421.
Sandradewi, J., Prévôt, A.S.H., Szidat, S., Perron, N., Alfarra, M.R., Lanz, V.A., Weingartner, E., Baltensperger, U., 2008. Using aerosol light absorption measurements for the quantitative determination of wood burning and traffic emission contributions to particulate matter. Environ. Sci. Technol. 42, 3316–3323. https://doi.org/10.1021/es702253m.
Slowik, J.G., Stainken, K., Davidovits, P., Williams, L.R., Jayne, J.T., Kolb, C.E., Worsnop, D.R., Rudich, Y., DeCarlo, P.F., Jimenez, J.L., 2004. Particle morphology and density characterization by combined mobility and aerodynamic diameter measurements. Part 2: application to combustion-generated soot aerosols as a function of fuel equivalence ratio. Aerosol Sci. Technol. 38, 1206–1222. https://doi.org/10.1080/027868290903916.
Souri, A.H., Choi, Y., Jeon, W., Kochanski, A.K., Diao, L., Mandel, J., Bhave, P.V., Pan, S., 2017. Quantifying the impact of biomass burning emissions on major inorganic aerosols and their precursors in the U.S. J. Geophys. Res. Atmos. 122 (12) https://doi.org/10.1002/2017JD026788, 020-12,041.
Sun, Y.L., Wang, Z.F., Fu, P.Q., Yang, T., Jiang, Q., Dong, H.B., Li, J., Jia, J.J., 2013. Aerosol composition, sources and processes during wintertime in Beijing, China. Atmos. Chem. Phys. 13, 4577–4592. https://doi.org/10.5194/acp-13-4577-2013.
Sylvestre, A., Mizzi, A., Mathiot, S., Masson, F., Jaffrezo, J.L., Dron, J., Mesbah, B., Wortham, H., Marchand, N., 2017. Comprehensive chemical characterization of industrial PM2.5 from steel industry activities. Atmos. Environ. 152, 180–190. https://doi.org/10.1016/j.atmosenv.2016.12.032.
Teinilä, K., Timonen, H., Aurela, M., Kuula, J., Rönkkö, T., Hellèn, H., Loukkola, K., Kousa, A., Niemi, J.V., Saarikoski, S., 2022. Characterization of particle sources and comparison of different particle metrics in an urban detached housing area. Finland. Atmos. Environ. 272, 118939 https://doi.org/10.1016/j.atmosenv.2022.118939.
Timonen, H., Carbone, S., Aurela, M., Saarnio, K., Saarikoski, S., Ng, N.L., Canagaratna, M.R., Kulmala, M., Kerminen, V.-M., Worsnop, D.R., Hillamo, R., 2013. Characteristics, sources and water-solubility of ambient submicron organic aerosol in springtime in Helsinki, Finland. Vienna, Austria J. Aerosol Sci., Special Issue: 10th International Conference on Carbonaceous Particles in the Atmosphere 56, 61–77. https://doi.org/10.1016/j.jaerosci.2012.06.005, 2011.
Tiwari, S., Chen, B., Singh, S., Singh, A.K., Srivastava, A.K., 2021. 5 - impacts of black carbon on environment and health. In: Hussain, C.M., Shukla, S.K., Joshi, G.M. (Eds.), Functionalized Nanomaterials Based Devices for Environmental Applications, Micro and Nano Technologies. Elsevier, pp. 107–125. https://doi.org/10.1016/B978-0-12-822245-4.00007-6.
Tsai, J.-H., Lin, K.-H., Chen, C.-Y., Ding, J.-Y., Choa, C.-G., Chiang, H.-L., 2007. Chemical constituents in particulate emissions from an integrated iron and steel facility. J. Hazard Mater. 147, 111–119. https://doi.org/10.1016/j.jhazmat.2006.12.054.
Ulbrich, I.M., Canagaratna, M.R., Zhang, Q., Worsnop, D.R., Jimenez, J.L., 2009. Interpretation of organic components from Positive Matrix Factorization of aerosol mass spectrometric data. Atmos. Chem. Phys. 9, 2891–2918. https://doi.org/10.5194/acp-9-2891-2009.
Uski, O., Jalava, P.I., Happo, M.S., Torvela, T., Leskinen, J., Mäki-Paakkanen, J., Tissari, J., Sippula, O., Lamberg, H., Jokiniemi, J., Hirvonen, M.-R., 2015. Effect of fuel zinc content on toxicological responses of particulate matter from pellet combustion in vitro. Sci. Total Environ. 511, 331–340. https://doi.org/10.1016/j.scitotenv.2014.12.061.
Varghese, C., H, G.L., Kalikeri, S., 2022. Understanding the status of important criteria air pollutants and its health effects – a review. International Journal of Health and Allied Sciences 11, 33–38. https://doi.org/10.55691/2278-344X.1006.
Visschedijk, A.H.J., Denier van der Gon, H.A.C., Hulskotte, J.H.J., Quass, U., 2013. Anthropogenic Vanadium emissions to air and ambient air concentrations in North-West Europe. E3S Web Conf 1, 03004. https://doi.org/10.1051/e3sconf/20130103004.
Wani, A.L., Ara, A., Usmani, J.A., 2015. Lead toxicity: a review. Interdiscipl. Toxicol. 8, 55–64. https://doi.org/10.1515/intox-2015-0009.
WHO, 2021. WHO Global Air Quality Guidelines: Particulate Matter ($PM_{2.5}$ and PM_{10}), Ozone, Nitrogen Dioxide, Sulfur Dioxide and Carbon Monoxide. World Health Organization. https://apps.who.int/iris/handle/10665/345329. License: CC BY-NC-SA 3.0 IGO.
WHO, 2022. World Health Statistics 2022: Monitoring Health for the SDGs, Sustainable Development Goals, 2022. World Health Organization, Geneva. Licence: CC BY-NC-SA 3.0 IGO.
Ye, Z., Liu, J., Gu, A., Feng, F., Liu, Y., Bi, C., Xu, J., Li, L., Chen, H., Chen, Y., Dai, L., Zhou, Q., Ge, X., 2017. Chemical characterization of fine particulate matter in Changzhou, China, and source apportionment with offline aerosol mass spectrometry. Atmos. Chem. Phys. 17, 2573–2592. https://doi.org/10.5194/acp-17-2573-2017.
Yin, L., Niu, Z., Chen, X., Chen, J., Zhang, F., Xu, L., 2014. Characteristics of water-soluble inorganic ions in PM2.5 and PM2.5–10 in the coastal urban agglomeration along the Western Taiwan Strait Region, China. Environ. Sci. Pollut. Res. 21, 5141–5156. https://doi.org/10.1007/s11356-013-2134-7.
Zhang, Q., Alfarra, M.R., Worsnop, D.R., Allan, J.D., Coe, H., Canagaratna, M.R., Jimenez, J.L., 2005. Deconvolution and quantification of hydrocarbon-like and oxygenated organic aerosols based on aerosol mass spectrometry. Environ. Sci. Technol. 39, 4938–4952. https://doi.org/10.1021/es048568l.
Zhao, Y., Gao, Y., 2008. Mass size distributions of water-soluble inorganic and organic ions in size-segregated aerosols over metropolitan Newark in the US east coast. Atmos. Environ. 42, 4063–4078. https://doi.org/10.1016/j.atmosenv.2008.01.032.
Zotter, P., Herich, H., Gysel, M., El-Haddad, I., Zhang, Y., Močnik, G., Hüglin, C., Baltensperger, U., Szidat, S., Prévôt, A.S.H., 2017. Evaluation of the absorption Ångström exponents for traffic and wood burning in the Aethalometer-based source apportionment using radiocarbon measurements of ambient aerosol. Atmos. Chem. Phys. 17, 4229–4249. https://doi.org/10.5194/acp-17-4229-2017.